CO Adsorption on Gold Clusters Stabilized on Ceria−Titania Mixed Oxides: Comparison with Reference Catalysts

Floriana Vindigni,[†] Maela Manzoli,[†] Anna Chiorino,[†] Tatyana Tabakova,[‡] and Flora Boccuzzi*,[†]

Department of Inorganic, Physical and Materials Chemistry and NIS Centre of Excellence, University of Turin, via P. Giuria 7, 10125 Turin, Italy, and Institute of Catalysis, Bulgarian Academy of Sciences, Acad. G. Bonchev Str., bl. 11, 1113 Sofia, Bulgaria

Received: July 10, 2006; In Final Form: September 6, 2006

Fourier transform infrared spectra of CO adsorption from 120 K up to room temperature on two gold catalysts supported on different mixed ceria−titania oxides are discussed in comparison with those obtained on Au/TiO_2 and Au/Fe_2O_3 reference catalysts provided by the World Gold Council. The spectra of adsorbed CO, run on the different samples before preliminary treatment, are shown and compared with those of the untreated catalysts and of the samples reduced either in CO or in hydrogen. Big differences have been found between the ceria−titania supported samples and the reference ones: unusual absorption bands, irreversible to outgassing, have been detected after CO interaction on the untreated and oxidized ceria containing samples. These absorptions are assigned to CO on Au_n^+ small clusters stabilized at the ceria defects. By reduction in hydrogen, negatively charged Au_n^- species are produced on the same sample. Oxidized small particles are present on the reference catalysts, but only on the untreated samples; after treatment, only metallic step sites are evident.

1. Introduction

The nature of the sites at the origin of the high activity of gold catalysts in different reactions at low temperature, such as CO oxidation, preferential CO oxidation, and water gas shift (WGS), is still a matter of debate. Uncoordinated gold step sites and borderline sites between the metal particles and the support are considered in many papers as the activation sites for CO.[1] However, it has been reported[2] that two atomic thickness gold layers fully covering a reducible oxide such as titania, without steps or borderline sites between the metal and the oxide, are very active in the CO oxidation reaction, suggesting that the activity of gold may be related not to the uncoordinated sites but to gold atoms spread on the reduced support and, possibly, bearing a partial negative charge as a consequence of an electron transfer from the support. Heiz and Schneider have shown that the extremely high catalytic activity of an eight-atom gold cluster supported on MgO is related to an electron transfer from the oxide surface to the metal cluster.[3] This effect is enhanced by the presence of oxygen vacancies that appear to be able to anchor the clusters and that also play an additional role, affecting the overall catalytic activity by the control of the negatively charged state of the gold clusters. In contrast, it has been reported[4] that mononuclear cationic gold complexes, even in the absence of metallic Au atoms, exhibit high catalytic activity in the same reaction. Moreover, Fu et al.,[5] on the basis of X-ray photoelectron spectroscopic data, suggested that in the water gas shift reaction on Au−ceria catalysts cationic gold is the catalytically active species and that metallic Au^0 particles do not take place in the reaction, as indicated by the similar activity observed on samples leached with a NaCN solution. Very recently, density functional theory (DFT) calculations and experimental data showed a relevant role of ultrasmall gold cationic clusters in the activity of gold catalysts in water gas shift reactions[6,7] and on the gas-phase hydrogen peroxide formation from H_2 and O_2.[8] A theoretical insight on O_2 and CO adsorption on neutral and positively charged gold clusters has been very recently reported.[9]

Moreover, it has been reported that the nature of the support on which gold is dispersed plays a crucial role in determining the catalytic activity. When Au nanoparticles are supported on ceria, the systems are very stable and exhibit a high activity for the WGS reaction over a wide temperature range.[10] The test of the ability in WGS and preferential CO oxidation on the new gold catalysts supported on CeO_2−TiO_2 mixed oxides with different ceria loadings (20% and 50%) has been undertaken and will be presented in the future.

To get a deeper understanding on the effect of the dispersion and of the oxidation state of gold on the chemisorption properties of some different catalysts, here we will discuss the Fourier transform infrared (FTIR) spectra of CO adsorption on two gold catalysts supported on mixed ceria−titania oxide, run at room temperature (RT) or at 120 K, in comparison with two reference samples, Au/TiO_2 and Au/Fe_2O_3, provided by the World Gold Council.[11] These last catalysts are currently the object of catalytic studies in different reactions, such as hydrogenation and WGS reactions, in many laboratories all over the world,[5,12,13] and our results may be useful for their interpretation.

2. Experimental Section

2.1. Materials. The Au/CeO_2−TiO_2 samples have been provided by the Institute of Catalysis, Bulgarian Academy of Sciences, Sofia, Bulgaria. The catalysts were prepared by the deposition−precipitation method of gold on CeO_2−TiO_2 supports suspended in water, via interaction of $HAuCl_4 \cdot 3H_2O$ and K_2CO_3 at a constant pH 7.0 and at a temperature of 333 K. After aging for 1 h, the precipitates were washed, dried in a vacuum at 353 K, and calcined under air at 673 K for 2 h. The

* Corresponding author. Telephone: +39 011 6707542. Fax: +39 011 6707855. E-mail: flora.boccuzzi@unito.it.
[†] University of Turin.
[‡] Bulgarian Academy of Sciences.

10.1021/jp064331v CCC: $33.50
Published on Web 10/19/2006

TABLE 1: Properties of the Examined Samples

sample	name	ceria:titania ratio	BET surface area (m^2/g)	preparation method	Au loading (wt %)	Au particle diameter (nm)
Au/CeO_2-TiO_2	AuCe0.5Ti0.5	50:50	104	DP[a]	3.00	$d \leq 2.0$
Au/CeO_2-TiO_2	AuCe0.2Ti0.8	20:80	77	DP[a]	3.00	$1.0 \leq d \leq 3.0$
Au/TiO_2	AuTi			DP[a]	1.51	3.8 ± 1.5[12]
Au/Fe_2O_3	AuFe			CP[b]	4.48	3.7 ± 0.93[12]

[a] DP, deposition−precipitation. [b] CP, coprecipitation.

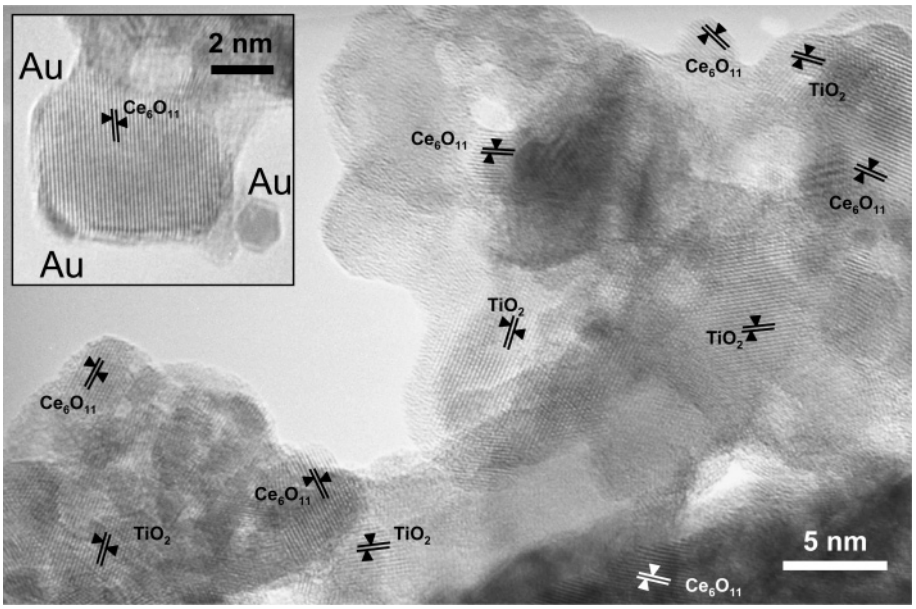

Figure 1. HRTEM image of AuCe0.5Ti0.5 evidencing the interdispersion of the two oxides. Inset: gold particles on a ceria crystalline nanoparticle. The image was taken at an original magnification of 800 000, while the inset was taken at an original magnification of 1 000 000.

gold loading for each catalyst was 3 wt %. The two mixed CeO_2-TiO_2 supports with a different ratio between ceria and titania, 50:50 and 20:80, respectively, were obtained by precipitation of cerium hydroxide on titania suspended in water by ultrasound. Aqueous solution of $Ce(NO_3)_3 \cdot 6H_2O$ and K_2CO_3 reacted under vigorous stirring at constant pH 9.0 and temperature 333 K. The resulting precipitates were aged at the same temperature for 1 h, and then were filtered and washed until removal of NO_3^- ions. After washing, the precipitates were dried in a vacuum at 353 K and calcined under air at 673 K for 2 h. The titania was lab-prepared by hydrolysis of $TiCl_4$ with ammonia at pH 9 and low temperature, washing until no Cl^- ions could be detected, and calcination at 673 K.

Au/Fe_2O_3 and Au/TiO_2 reference catalysts provided by the World Gold Council[14] have also been examined. The main features of the samples are summarized in Table 1.

2.2. Methods. The syntheses of the supports and of the gold catalysts were carried out in a "Contalab" laboratory reactor enabling complete control of the reaction parameters (pH, temperature, stirrer speed, reactant feed flow, etc.) and high reproducibility.

High-resolution transmission electron microscopic (HRTEM) analysis was performed on the AuCeTi catalyst using a JEOL JEM 2010 (200 kV) microscope equipped with an EDS analytical system Oxford Link. The powdered sample was ultrasonically dispersed in isopropyl alcohol, and the obtained suspension was deposited on a copper grid, coated with a porous carbon film.

Specific surface area was performed by N_2 adsorption at 77 K with a traditional BET volumetric apparatus.

FTIR spectra were taken on a Perkin-Elmer 1760 spectrometer (equipped with a MCT detector) with the samples in self-supporting pellets introduced in a cell allowing thermal treatments in controlled atmospheres and spectrum scanning at controlled temperatures (from 120 to 300 K). Band integration was carried out by "Curvefit", in Spectra Calc (Galactic Industries Co.) by means of Lorentzian curves. From each spectrum, the spectrum of the sample before the inlet of CO was subtracted. The spectra were normalized respect to the gold content of each sample.

3. Results and Discussion

3.1. BET, X-ray Diffraction, and TEM Characterization of the Catalysts. We performed BET measurements on both ceria−titania supported samples, and we compared them with the specific surface area of the pure titania support, which is 86 m^2/g. Looking at these data, it can be observed that the AuCe0.5Ti0.5 catalyst has a specific surface area significantly higher than that of titania itself, while the specific surface area of the AuCe0.2Ti0.8 is very close to that of pure titania. These features can be explained looking at the HRTEM measurements that point out quite different morphologies and structures of the supports. On the AuCe0.5Ti0.5 catalyst (Figure 1), a large interdispersion of ceria and titania is evident and a careful analysis of the diffraction fringes of the two oxides reveals the presence also of substoichiometric phases such as Ce_6O_{11}. Ceria appears as highly crystalline nanoparticles round in shape and with an average diameter around 4.5 nm, while the titanium oxide particles appear larger. Therefore, on this sample the cerium oxide is responsible for the higher specific surface, being 50% of the support and being smaller than titania.

On AuCe0.2Ti0.8 two distinct regions, easily recognizable, are evidenced: the former, appearing darker, composed mainly

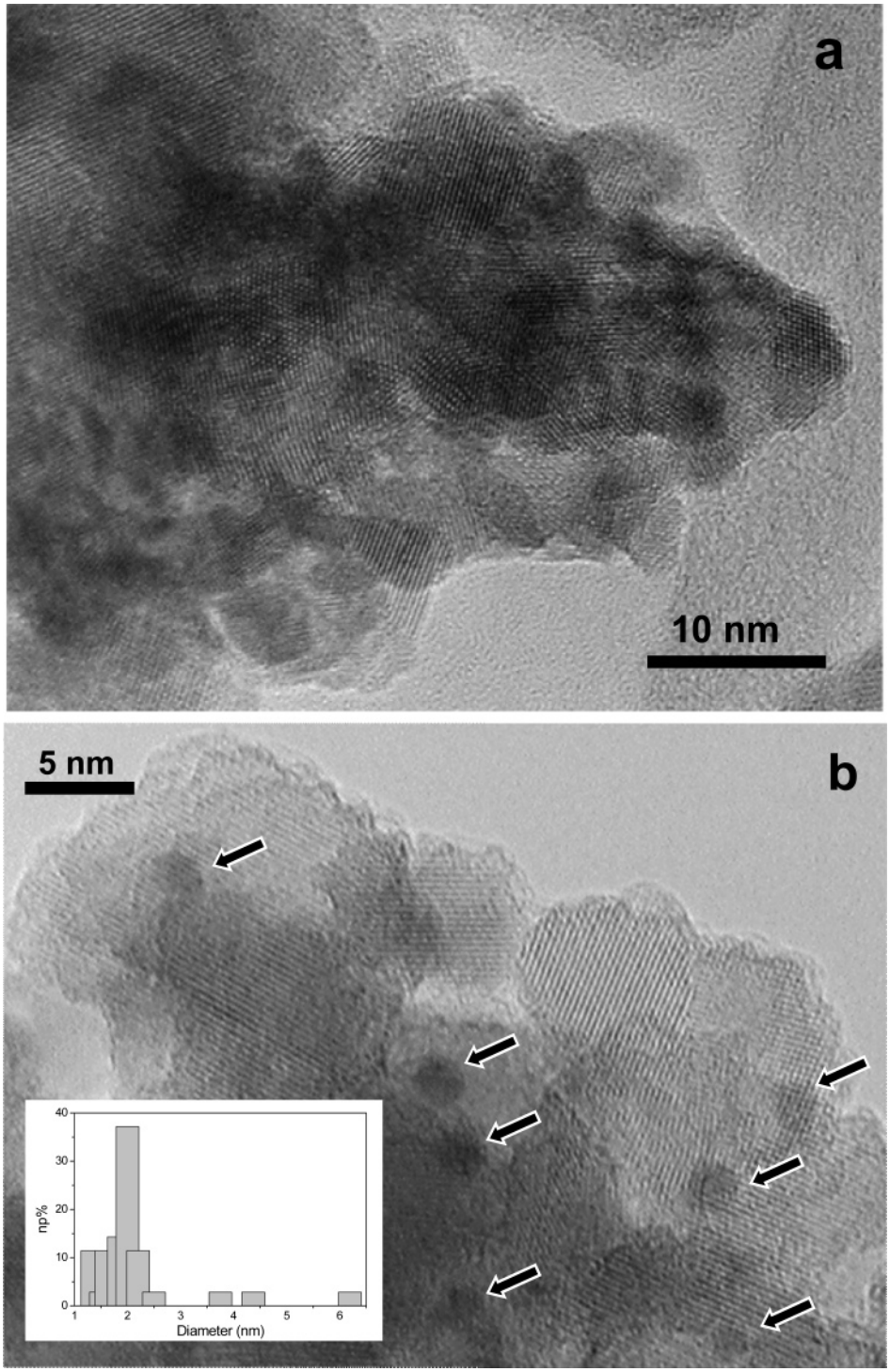

Figure 2. HRTEM images of AuCe0.2Ti0.8 sample: gold particles on a CeO_2-rich region (a) and on a TiO_2-rich region (b). Inset in (b): size distribution of Au particles for the AuCe0.2Ti0.8 sample shown in the HRTEM images. Both image a and image b were taken at an original magnification of 500 000.

of ceria (Figure 2a) and the latter composed mainly of titania (Figure 2b). The analysis of the diffraction fringes shows regular planes exposed by the two oxides, and ceria particles appear larger than in the AuCe0.5Ti0.5 sample. As a consequence, on AuCe0.2Ti0.8 the presence of the ceria does not have a positive effect on the specific surface area that is close to that of pure titania.

Moreover, HRTEM evidences also gold particles, but with different ease and definition on the two catalysts. Because of the small difference in the atomic weight, it is difficult to distinguish the gold metal from CeO_2. As a consequence, on the AuCe0.5Ti0.5 catalyst (Figure 1), the most rich in ceria, only a few gold particles, with size around 2 nm, have been observed (inset of Figure 1), suggesting that most of the gold escapes the TEM detection. On AuCe0.2Ti0.8 catalyst, gold particles are hardly observable on the ceria-rich region (Figure 2a), while they are easily seen as dark contrasts on the surface of the titania-rich region, as evidenced by the arrows in the image reported in Figure 2b. The average diameter of the gold particles was extimated to be $\approx$2 nm, with the particle size distribution being in the 1−3 nm range (inset of Figure 2b).

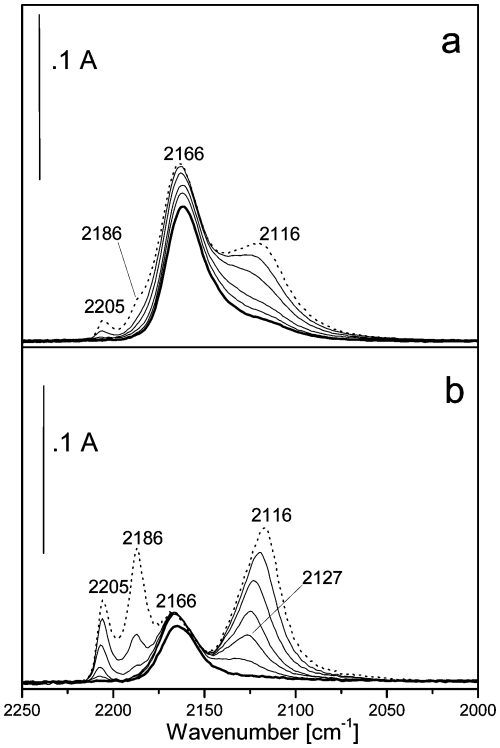

Figure 3. FTIR spectra of AuCe0.5Ti0.5 (a) and AuCe0.2Ti0.8 (b) oxidized at 673 K after the adsorption of 15 mbar of CO at RT (dashed line), at decreasing pressures (fine lines), and under outgassing at RT (bold line).

As for the reference samples, looking at the data reported in the sheets provided by the World Gold Council, both catalysts show the same average diameter of gold particles (see Table 1), but the size distribution is quite different, broader for AuTi, 3.8 ± 1.5, than for AuFe, 3.7 ± 0.93. The effects of this different size distribution will be discussed in the analysis of the FTIR spectra of CO adsorbed at 120 K (section 3.3).

3.2. FTIR Spectra of Gold Catalysts Supported on Ceria−Titania Mixed Oxides. Figure 3 shows the FTIR spectra produced by the adsorption of 15 mbar of CO at RT and at decreasing coverages at the same temperature on AuCe0.5Ti0.5 (Figure 3a) and on AuCe0.2Ti0.8 (Figure 3b), both samples having been previously oxidized at 673 K. Besides the usual bands related to CO on the support and on metallic gold that will be discussed later on, an unusual and broad absorption band at 2166 cm^{-1} is observed for both catalysts. This band is almost completely irreversible to the outgassing at RT, giving evidence of a strong bond between CO and the involved adsorption sites. A CO absorption band that is irreversible at RT has never been observed before on supported gold, and this feature needs some comments. Looking at the paper of Wu et al.,[15] where DFT calculations of carbon monoxide adsorption on small cationic, neutral, and anionic clusters are shown, an assignment of that absorption can be made. The authors reported that the adsorption energies of CO on the cationic clusters are greater than those on the neutral and anionic complexes and also the calculated CO vibrational frequencies are larger than on neutral clusters. Very recently, Fielicke et al.[16] estimated experimentally the CO vibrational frequencies of $Au_n(CO)_m^+$ complexes in the gas phase, where $3 \leq n \leq 10$ and $3 \leq m \leq 8$. In particular, they observed that the ν_{CO} decreases when the nuclearity of the gold clusters increases. Looking at these results, the absorption centered at about 2166 cm^{-1} may be related to CO adsorbed on cationic gold clusters, stabilized on the mixed oxide surface. It is well-known that the most stable gold carbonyls are those of the Au^+ cations. This is due to the bonding of CO to cationic gold sites by σ-bonds and π-back-bonds. The increase of the effective charge of the gold sites reflects in a strengthening of the σ-bond and in an increase of the CO stretching frequency. The π-back-donation should lead to some decrease of the CO stretching frequency and also to an increase of the overall bond strength. However, the increase of the effective charge of the cation alone should reflect in the decrease of the π-bond order. A detailed analysis of these effects has been provided for the Cu^+-CO and Ag^+-CO systems.[17] It has been concluded that the π-bond for the Cu^+-CO system is only slightly enhanced with the increase of the effective charge of the cation. In the case of Au^+, where the π-back-donation is less important than for the Cu^+ cations, the change of the π-bond order should be even weaker. Hence, the stability and the frequency of the Au^+-CO species can well be interpreted using the conception of the covalent σ-bond alone. It may be relevant to observe that also cationic copper binds CO irreversibly at room temperature, differently from metallic copper.

The band at 2166 cm^{-1} shows a different intensity in the two samples: in particular, it is more intense for AuCe0.5Ti0.5 (Figure 3a) than for AuCe0.2Ti0.8. The intensity ratio of the band at 2166 cm^{-1} in the two samples is close to 3. This feature indicates that on AuCe0.5Ti0.5 the gold clusters are more abundant than on AuCe0.2Ti0.8; i.e., their abundance appears related to the amount of ceria in the samples. Possibly the gold clusters are stabilized by interaction with nanodispersed ceria. Interestingly, we already observed a band in a similar position, showing quite similar features under the same experimental conditions, after CO adsorption on gold catalysts supported on ceria modified by the insertion of lanthanum.[18] It can be supposed that the stabilizing effect of the lanthanum doping is the same obtained by mixing the two oxides.

The band at 2116 cm^{-1} is due to CO molecules adsorbed on Au sites; its frequency can be taken as an indication that the sites are partially oxidized.[19] It has been observed by Bondzie et al.[20] that Au particles with size below 2 nm are able to bind oxygen. As confirmed by HRTEM, most of the gold particles are very small.

We observe that the ratio between the integrated areas of the 2116 cm^{-1} band for AuCe0.2Ti0.8 and for AuCe0.5Ti0.5 is 1.3, indicating that the amount of sites exposed at the surface of the small metallic gold particles is, to some extent, larger on the 20:80 sample than on the 50:50 sample.

As for the absorptions observed at higher frequencies, two bands are evident for both samples at 2205 and 2186 cm^{-1} (Figure 3); they are more intense for AuCe0.2Ti0.8. The two bands are assigned to CO adsorbed on Ti^{4+} surface sites, with the first band to the most uncoordinated ones and the second band to ions exposed on regular (001) or (010) planes.[21,22] The ceria deposition in the AuCe0.5Ti0.5 sample seems to strongly perturb the titania sites, both the most uncoordinated and those exposed on regular planes.

After reduction in hydrogen at 473 K, the band at 2166 cm^{-1} is totally depleted for both samples, as shown in Figure 4, where the FTIR spectra of CO adsorption at RT on the AuCe0.5Ti0.5 (Figure 4a) and AuCe0.2Ti0.8 (Figure 4b) reduced catalysts are reported. This feature can support the assignment to the cationic gold clusters, present only at the surface of the oxidized samples. As for the bands at 2205 and at 2186 cm^{-1}, due to CO adsorbed on Ti^{4+} ions more or less uncoordinated, the intensities strongly depend on the effectiveness of the pretreatment.

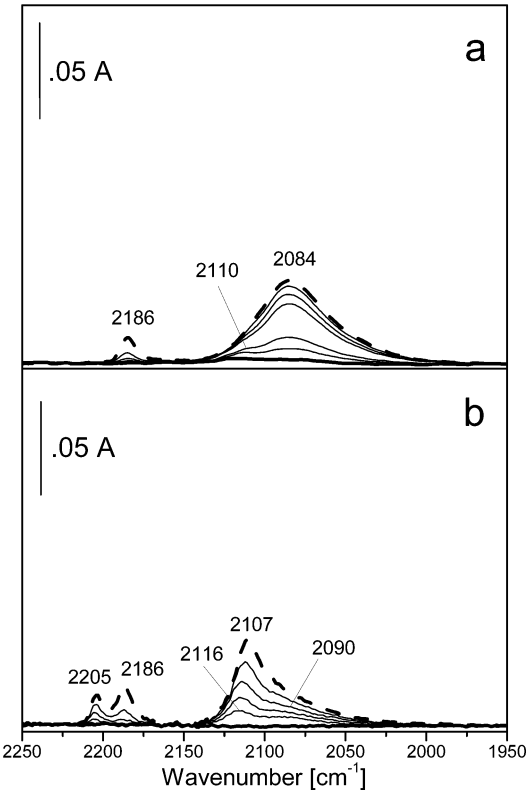

Figure 4. FTIR spectra of AuCe0.5Ti0.5 (a) and AuCe0.2Ti0.8 (b) reduced in H_2 at 473 K after the adsorption of 15 mbar of CO at RT (dashed line), at decreasing pressures (fine lines), and under outgassing at RT (bold line).

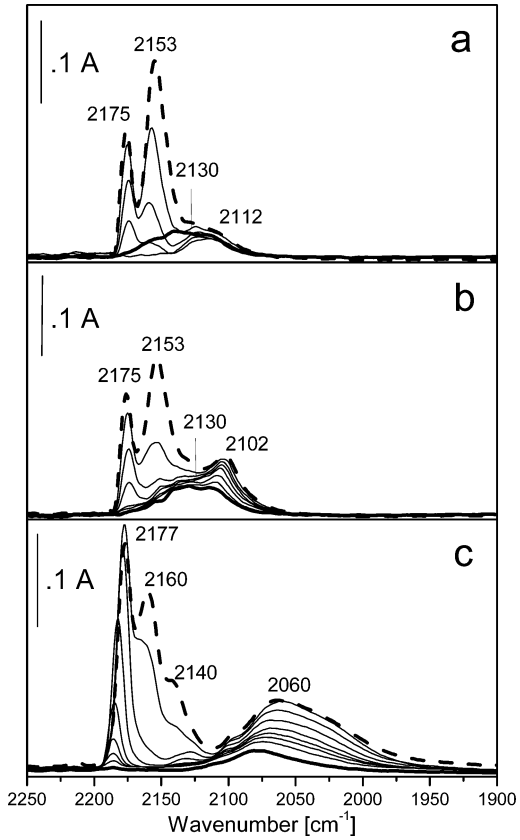

Figure 5. FTIR spectra of AuCe0.5Ti0.5 as received (a), reduced in CO at RT (b), and reduced in H_2 at 473 K (c) after the adsorption of 0.5 mbar of CO at 120 K (dashed line) and at increasing temperature (fine lines) up to RT (bold line).

The main feature here observed related to CO interacting with gold sites is a broad band at 2084 cm^{-1} for AuCe0.5Ti0.5 (Figure 4a). It has been stressed, in the discussion of the HRTEM data, that most of the gold cannot be seen. The FTIR observation can be taken as an indirect indication that gold is highly dispersed and in good contact with the small ceria particles, from which it cannot be distinguished clearly, as a consequence of the poor difference in the contrast. The small ceria particles, after the reductive treatments, are not fully stoichiometric and can produce an electron transfer from Ce^{3+} to Au. Therefore, the band is red shifted with respect to the usual position of CO adsorbed on Au^0 step sites, at 2100 cm^{-1}.[19] On the basis of our previous results on other gold catalysts supported on ceria,[23] we can infer that the shift toward the low-frequency side is an indication that, on AuCe0.5Ti0.5, negatively charged clusters or flattened, thin gold particles are present at the surface of defective ceria. These particles cannot be easily recognized, and most of them escape TEM detection (see inset of Figure 1, where two flattened particles are observed). It has been reported that nanosized ceria shows higher activity than bulk phases because of the easier reducibility.[24] The presence of these defects stabilizes the highly dispersed gold species, differently from other samples, such as the reference ones, which will be discussed later on. It can be proposed that, after reduction, Au spreads on the reduced ceria and the three-dimensional gold particles, possibly present before the reductive treatment, may become very thin films. Akita et al.[25] studied by HRTEM the gold nanoparticles supported on a model CeO_2 exposing low index flat faces, typically in the {111} and {100} planes, to overcome the problem of the poor difference in contrast between the two phases and of the consequent difficulty in detecting the gold particles on ceria. The authors observed that the smallest and thin gold nanoparticles disappeared under the beam and in a vacuum, shrinking layer by layer down to a monatomic layer. A similar phenomenon may occur also by reducing our samples in H_2 at 473 K, in a more evident way on AuCe0.5Ti0.5, where the cerium oxide loading is higher and the gold particles are smaller and flattened. This phenomenon was observed for Cu/ZnO catalysts in reducing reaction atmosphere[26] by in situ HRTEM. Therefore, we can conclude that, on the AuCe0.5Ti0.5 catalyst, most of the gold is dispersed on ceria rather than on titania. Only a small fraction of the gold is present as tridimensional particles as indicated by the weak band at 2110 cm^{-1} (Figure 4a), assigned to CO adsorbed on Au^0 step sites.

By contrast, on the AuCe0.2Ti0.8 catalysts, a fraction of the gold particles, possibly in contact with titania, does not suffer in the reducing atmosphere, as indicated by the presence of the usual band (at 2107 cm^{-1}) and by the dark dots evidenced by arrows in the TEM images. The remaining gold is in contact with ceria, and it is small enough to be negatively charged and flattened after reduction, as demonstrated by the presence of the shoulder at 2090 cm^{-1}. In conclusion, depending on the thermal pretreatment and on the support, the CO interaction at RT well evidenced the presence of cationic clusters, or metallic gold particles, or small negatively charged flat particles.

We also performed experiments of CO adsorption starting from 120 K, to characterize the surface composition of the as-prepared catalysts.

The FTIR spectra after CO adsorption at 120 K on AuCe0.5Ti0.5 simply outgassed at RT (as-received sample) are reported in Figure 5a. A second adsorption of CO at 120 K was performed on the same sample reduced in CO, i.e., after the gradual heating to RT in CO atmosphere. The catalyst was

then kept again in CO atmosphere during the second increase of temperature up to RT. These experiments are shown in Figure 5b.

We adsorbed CO at low temperature also on the AuCe0.2Ti0.8 sample, both as received and reduced in CO. We will not report these spectra since they are very similar to those obtained for the AuTi reference catalyst that will be shown in the next paragraph, such as for the nature, the position, and the intensity of the bands related to the species present at the surface.

The spectra reported in Figure 5 clearly evidence the changes produced on the surface composition by interacting with CO from 120 K up to RT. The dashed line of Figure 5a is related to the adsorption of 0.5 mbar of CO at 120 K on the as-received AuCe0.5Ti0.5 sample.

Beside the bands at 2175 cm^{-1}, due to CO on Ti^{4+} cations,[21,22] and at 2153 cm^{-1} related to CO interacting with the OH groups and with the Ce^{x+} ions of the support,[27] a broad absorption at 2112 cm^{-1} is produced after CO adsorption at 120 K. This band can be related to the presence of partially oxidized gold.[18] By increasing the temperature (fine lines) up to RT (bold line), the peaks at higher frequency decrease in intensity and then disappear, while the band at 2112 cm^{-1} does not change its intensity. Interestingly, a broad absorption with a maximum at 2130 cm^{-1} increased at RT (bold line).

Further contact with CO at RT is necessary to evidence Au^0 sites. In fact, by cooling to 120 K in the same atmosphere, a band at 2102 cm^{-1}, due to CO on Au^0 sites, is observed (Figure 5b) and overlapped the absorption bands already observed during the first interaction with the CO molecule. The intensification of the 2102 cm^{-1} band is an indirect indication that, on the as-received sample, most of the gold particles are covered by adsorbed oxygen, as a consequence of their small size. This phenomenon has been highlighted for Au particles with size below 2 nm.[19,20] We can assume that on this catalyst the oxygen initially covering the ultrasmall gold particles is removed by the reductive interaction with CO that makes the gold step sites available to adsorption, as confirmed by the increase of the band at 2102 cm^{-1} detected by cooling again to 120 K in CO.

The broad band with a maximum at 2130 cm^{-1} remains after heating to RT in 0.5 mbar of CO (Figure 5b, bold line), in the same position as that of the band already observed for the as-received sample (Figure 5a, bold line). This absorption is not reversible to the prolonged outgassing at RT, which is an indication of a quite strong interaction between CO and the related sites.

On the basis of the observed behavior, we can assume that the band at 2130 cm^{-1} is again related to CO on small cationic gold clusters, possibly stabilized at the mixed oxide interface.

The spectra related to the same sample, mildly reduced in hydrogen at 473 K and cooled to 120 K, look quite different (Figure 5c). The band at 2102 cm^{-1} and the broad absorption in the 2130 cm^{-1} region are totally lacking and are actually substituted by a broad absorption with a maximum at 2060 cm^{-1} extending from 2100 to 1950 cm^{-1} (dashed line). This absorption, very similar to that previously observed after CO adsorption at RT on the same reduced sample (Figure 4a), has been assigned to CO adsorbed on very small clusters or very thin gold particles, possibly negatively charged by the charge transfer from the reduced ceria.

3.3. Gold Reference Catalysts. *3.3.1. Au/TiO_2.* The adsorption of 0.5 mbar of CO at 120 K on the as-received reference catalyst (Figure 6a, dashed line) does not reveal at all the typical band at 2100 cm^{-1} related to the chemisorption on Au^0 sites usually observed by us and other authors.[28,29] On the contrary,

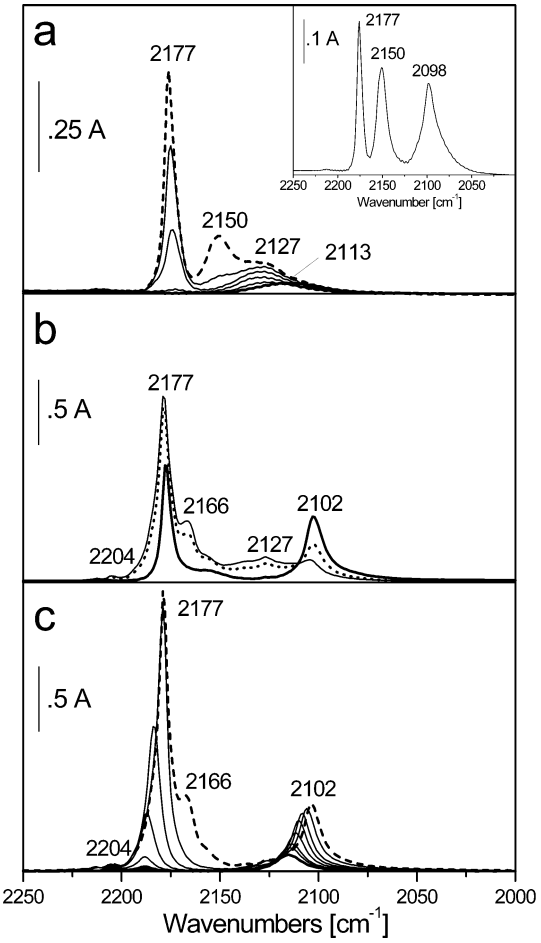

Figure 6. (a) FTIR spectra of as-received AuTi after the adsorption of 0.5 mbar of CO at 120 K (dashed line) and at increasing temperature (fine lines) up to RT (bold line). Inset: FTIR spectrum of AuTi previously reduced in CO after the adsorption of 0.5 mbar of CO at RT and cooling to 120 K. (b) FTIR spectra of AuTi oxidized at 673 K after the adsorption of 0.5 mbar of CO at 120 K (fine line) and after further interactions with CO from 120 K up to RT (dotted and bold lines). (c) FTIR spectra of AuTi reduced in H_2 at 523 K after the adsorption of 0.5 mbar of CO at 120 K (dashed line) and at increasing temperature (fine lines) up to RT (bold line).

a broad absorption at about 2127 cm^{-1} is observed. In addition, bands at 2177 and 2150 cm^{-1}, due to the interaction of CO with Ti^{4+} [21,22] and OH groups, respectively, are also present.

Upon heating in CO atmosphere up to RT (fine lines), the peak at higher frequency decreases in intensity and then disappears, while the band at 2150 cm^{-1} is easily depleted already in the first stages of the increase of the temperature. The absorption centered at 2127 cm^{-1} gradually reduces in intensity, and a weak and broad band at 2113 cm^{-1} is still present at RT (bold line). These last two bands behave toward heating in CO differently from the bands at 2130 and at 2112 cm^{-1} for the AuCe0.5Ti0.5 sample.

After further contact with CO at RT the usual Au^0 sites are produced. In fact, by cooling to 120 K in the same atmosphere, an intense and quite symmetric band at 2098 cm^{-1}, due to CO on Au^0 sites, is observed (inset in Figure 6a). This is the same phenomenon previously discussed for the as-received AuCe0.5Ti0.5 sample: also in this case the gold particles are initially ultrasmall and covered by oxygen.[19,20] The difference now is that a reductive interaction with CO is able not only to remove oxygen, but also to push the smallest particles to coalesce. The coalescence occurs on this AuTi sample and not

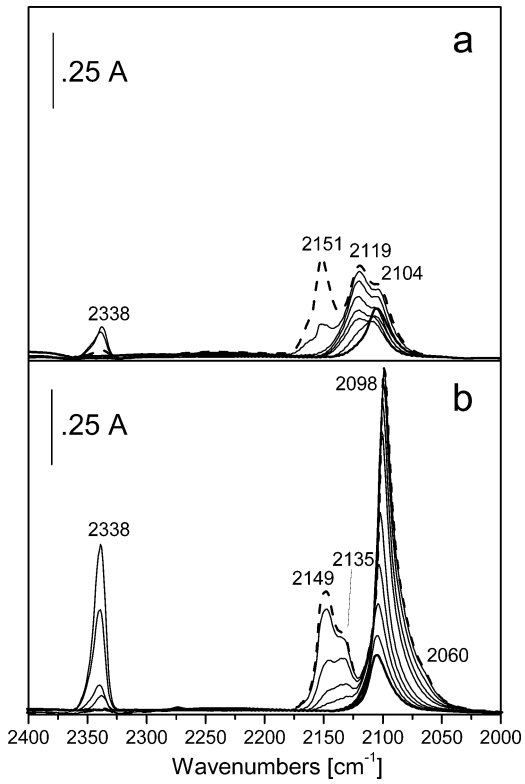

Figure 7. FTIR spectra of AuFe as received (a) and reduced in CO at RT (b) after the adsorption of 0.5 mbar of CO at 120 K (dashed line) and at increasing temperature (fine lines) up to RT (bold line).

on the AuCe0.5Ti0.5 one, as a consequence of the interaction with the defective and highly dispersed ceria.

However, even if the large majority of the ultrasmall gold particles coalesce to "conventional" particles (whose size, obtained by HRTEM measurements, is reported in Table 1) after the reductive interaction with the CO molecule at RT, some of them are still present after an oxidation treatment at 673 K. Besides the bands at 2204, 2177, and 2166 cm^{-1}, produced by CO adsorption at 120 K (Figure 6b, fine line) and already assigned to CO on different cationic sites of the support,[21,22] we observe again the band at 2127 cm^{-1}. At the same time, the band at 2102 cm^{-1} related to CO on Au^0 increases in intensity after subsequent interactions with CO from 120 K up to RT (dotted and bold lines).

On the basis of these features, as on AuCeTi, the band at 2127 cm^{-1} can be assigned also in this case to CO on small cationic clusters.[15] Moreover, similarly to what is observed on the AuCeTi samples, the band at 2127 cm^{-1} is not detected at all after the adsorption of CO at 120 K if the AuTi catalyst is submitted to a reduction at 523 K in hydrogen (Figure 6c, dashed line).

From these results it appears that there are almost no clean, gold metallic particles of 3−4 nm diameter on the as-received AuTi reference catalyst, but some of these particles are produced either by interaction with CO at RT during the FTIR experiments or by the electron beam during the HRTEM measurements performed by the manufacturer.

3.3.2. Au/Fe_2O_3. The adsorption of 0.5 mbar of CO at 120 K on as-received AuFe (Figure 7a, dashed line) produced bands at 2151, 2119, and 2104 cm^{-1}. During the temperature increase (fine lines) up to RT (bold line), the band at 2151 cm^{-1}, assigned to CO in interaction with the OH groups of the support, is easily depleted. At the same time, the band at 2119 cm^{-1} gradually reduces its intensity and it is finally depleted. At 253 K, an isosbestic point at 2111 cm^{-1} is evident, indicating that a conversion of the species related to the band at 2119 cm^{-1} into a new one, responsible for the band at 2104 cm^{-1}, has occurred during the gradual increase of temperature. Differently from the AuCeTi samples and from the AuTi reference sample illustrated previously, a fraction of the gold particles is clean, not covered by oxygen, while another fraction appears partially oxidized.[19,20] Again, by interaction with the CO molecule at increasing temperature, oxygen is removed and Au^0 sites are produced, as confirmed by the presence of the isosbestic point at 2111 cm^{-1}. At the same time, some CO_2 is produced, as indicated by the increase of a band at 2338 cm^{-1}. This hypothesis is further strengthened by the experiments made on the same sample by contacting it with CO at RT: in this case only a band at 2104 cm^{-1} is evident (not shown).

The second adsorption of 0.5 mbar of CO at 120 K on AuFe, now reduced in CO, is reported in Figure 7b (dashed line). A band at 2149 cm^{-1}, due to CO on OH groups, weak bands at 2135 and 2060 cm^{-1}, assigned to CO adsorbed on Fe^{x+} cations of the support,[17] and a defined band at 2098 cm^{-1}, due to CO on Au^0 sites, are observed. The last one shows the usual behavior of the band of CO on metallic gold,[30] such as the intensity and the frequency, by decreasing the coverage.

After the second interaction with CO the band at 2098 cm^{-1} is much more intense than the 2104 cm^{-1} one observed on as-received AuFe (Figure 7a, dashed curve): the ratio between the integrated areas of the bands is equal to 4.8. On the as-received AuFe reference catalyst the majority of gold particles are initially very small and, analogous to what is observed for AuTi, possibly agglomerate into bigger ones under the electron beam of the microscope (hence explaining the size distribution reported in Table 1) and during the heating in CO atmosphere from 120 K up to RT. The coalescence of the ultrasmall particles occurs more easily when the surface oxygen is removed by CO producing CO_2. The produced CO_2 reaches maximum intensity at about 140 K, and it is more intense than the amount observed during the first increase of temperature. The mean diameters of the gold particles and the standard deviations, determined by TEM, are 3.8 ± 0.75 nm for Au/TiO_2 and 3.7 ± 0.47 nm for Au/Fe_2O_3. Therefore, despite the similar average particle sizes of the two reference samples, the different size distributions can justify the observed spectroscopic differences.

4. Final Remarks

FTIR evidence of clusters and ultrasmall gold particles has been reported. CO adsorption on the four different gold catalysts showed that the nature of the exposed sites and the strength of the absorption are different.

(i) Special sites where CO is irreversibly bonded to the outgassing at RT, ascribed to small cationic clusters, have been evidenced on both oxidized Au/CeO_2-TiO_2 catalysts, characterized by a band at 2166 cm^{-1}.

(ii) Only very highly dispersed and partially oxidized gold particles, adsorbing CO reversibly at RT, are present on the two oxidized reference catalysts.

(iii) On the reduced Au/CeO_2-TiO_2 catalysts, mainly on the 50:50 sample, negatively charged clusters or flattened, thin gold particles, characterized by a band at 2084 cm^{-1}, are present.

(iv) On the reduced reference catalysts the usual absorption band of CO adsorbed on metallic step sites at 2098 cm^{-1} is detected.

Taking into account that the four characterized gold catalysts are very active in low-temperature CO oxidation, the clusters and/or the very small gold particles, not detectable by HRTEM

and evidenced by FTIR in this work, may be the most relevant species in the reactions involving CO.

Acknowledgment. The Ministero dell'Istruzione, dell'Università e della Ricerca Scientifica, is gratefully acknowledged for financial support in Project Nos. 2003035534_004 (PRIN2003) and 2004038984_005 (PRIN2004).

References and Notes

(1) Bond, G. C.; Thompson, D. T. *Catal. Rev.—Sci. Eng.* **1999**, *41*, 319 and references therein.
(2) Chen, M. S.; Goodman, D. *Science* **2004**, *306*, 5694.
(3) Heiz, U.; Schneider, W. D. *J. Phys. D: Appl. Phys.* **2000**, *33*, R85.
(4) Fierro-Gonzales, J. C.; Gates, B. C. *J. Phys. Chem. B* **2004**, *108*, 16999.
(5) Fu, Q.; Deng, W.; Saltsburg, H.; Flytzani-Stephanopoulos, M. *Appl. Catal., B: Environ.* **2005**, *56*, 57.
(6) Liu, Z.-P.; Jenkins, S. J.; King, D. A. *Phys. Rev. Lett.* **2005**, *94*, 196102.
(7) Tibiletti, D.; Amieiro-Fonseca, A.; Burch, R.; Chen, Y.; Fisher, J. M.; Goguet, A.; Hardacre, C.; Hu, P.; Thompsett, D. *J. Phys. Chem. B* **2005**, *109*, 22553.
(8) Joshi, A. M.; Delgass, W. N.; Thomson, K. T. *J. Phys. Chem. B* **2005**, *109*, 22392.
(9) Prestianni, A.; Martorana, A.; Labat, F.; Ciofini, I.; Adamo, C. *J. Phys. Chem. B* **2006**, *110*, 12240.
(10) Tabakova, T.; Boccuzzi, F.; Manzoli, M.; Sobczak, J. W.; Idakiev, V.; Andreeva, D. *Appl. Catal., B: Environ.* **2004**, *49*, 73.
(11) Gold reference catalysts. *Gold Bull.* **2003**, *36*, 1.
(12) Abad, A.; Concepciòn, P.; Corma, A.; Garcìa, H. *Angew. Chem., Int. Ed.* **2005**, *44*, 4066.
(13) Milone, C.; Ingoglia, R.; Schipilliti, L.; Crisafulli, C.; Neri, G.; Galvagno, S. *J. Catal.* **2005**, *236*, 80.
(14) Samples number 17C and 20A, supplied by World Gold Council; www.gold.org.
(15) Wu, X.; Senapati, L.; Nayak, S. K.; Selloni, A.; Hajaligol, M. *J. Chem. Phys.* **2002**, *117*, 4010.
(16) Fielicke, A.; von Helden, G.; Meijer, G.; Pedersen, D. B.; Simard, B.; Rayner, D. M. *J. Am. Chem. Soc.* **2005**, *127*, 8416.
(17) Hadjiivanov, K. I.; Vayssolv, G. N. *Adv. Catal.* **2002**, *47*, 307.
(18) Manzoli, M.; Boccuzzi, F.; Chiorino, A.; Vindigni, F.; Deng, W.; Flytzani-Stephanopoulos, M. *J. Catal.*, in press.
(19) Boccuzzi, F.; Chiorino, A.; Manzoli, M.; Lu, P.; Akita, T.; Ichikawa, S.; Haruta, M. *J. Catal.* **2001**, *202*, 256.
(20) Bondzie, V. A.; Parker, S. C.; Campbell, C. T. *Catal. Lett.* **1999**, *63*, 143.
(21) Morterra, C. *J. Chem. Soc., Faraday Trans. 1* **1988**, *84*, 1617.
(22) Martra, G. *Appl. Catal., A: Gen.* **2000**, *200*, 275.
(23) Tabakova, T.; Boccuzzi, F.; Manzoli, M.; Andreeva, D. *Appl. Catal., A: Gen.* **2003**, *252*, 385.
(24) Carrettin, S.; Corma, A.; Iglesias, M.; Sánchez, F. *Appl. Catal., A: Gen.* **2005**, *291*, 247.
(25) Akita, T.; Okumura, M.; Tanaka, K.; Kohyama, M.; Haruta, M. *J. Mater. Sci.* **2005**, *40*, 3101.
(26) Hansen, P. L.; Wagner, J. B.; Helveg, S.; Rostrup-Nielsen, J. R.; Clausen, B. S.; Topsøe, H. *Science* **2002**, *295*, 2053.
(27) Binet, C.; Daturi, M.; Lavalley, J. C. *Catal. Today* **1999**, *50*, 207.
(28) Menegazzo, F.; Manzoli, M.; Chiorino, A.; Boccuzzi, F.; Tabakova, T.; Signoretto, M.; Pinna, F.; Pernicone, N. *J. Catal.* **2006**, *237*, 431.
(29) Derrouiche, S.; Gravejat, P.; Bianchi, D. *J. Am. Chem. Soc.* **2004**, *126*, 13010.
(30) Manzoli, M.; Chiorino, A.; Boccuzzi, F. *Oxide Based Materials*; Gamba, A., Colella, C., Coluccia, S., Eds.; Studies in Surface Science and Catalysis 155; Elsevier: New York, 2005; p 405 and references therein.